Document made available under the Patent Cooperation Treaty (PCT)

International application number: PCT/GB04/005185

International filing date: 13 December 2004 (13.12.2004)

Document type: Certified copy of priority document

Document details: Country/Office: GB
Number: 0425254.0
Filing date: 16 November 2004 (16.11.2004)

Date of receipt at the International Bureau: 02 May 2005 (02.05.2005)

Remark: Priority document submitted or transmitted to the International Bureau in compliance with Rule 17.1(a) or (b)

PCT/GB 2004 / 0 0 5 1 8 5

The Patent Office
Concept House
Cardiff Road
Newport
South Wales
NP10 8QQ

INVESTOR IN PEOPLE

I, the undersigned, being an officer duly authorised in accordance with Section 74(1) and (4) of the Deregulation & Contracting Out Act 1994, to sign and issue certificates on behalf of the Comptroller-General, hereby certify that annexed hereto is a true copy of the documents as originally filed in connection with the patent application identified therein.

In accordance with the Patents (Companies Re-registration) Rules 1982, if a company named in this certificate and any accompanying documents has re-registered under the Companies Act 1980 with the same name as that with which it was registered immediately before re-registration save for the substitution as, or inclusion as, the last part of the name of the words "public limited company" or their equivalents in Welsh, references to the name of the company in this certificate and any accompanying documents shall be treated as references to the name with which it is so re-registered.

In accordance with the rules, the words "public limited company" may be replaced by p.l.c., plc, P.L.C. or PLC.

Re-registration under the Companies Act does not constitute a new legal entity but merely subjects the company to certain additional company law rules.

Signed Stephen Hordley

Dated 19 April 2005

17NOV04 E941820-1 D10005
P01/7700 0.00-0425254.0 ACCOUNT CHA

1/77

Patents Form 1/77

Patents Act 1977
(Rule 16)

The Patent Office

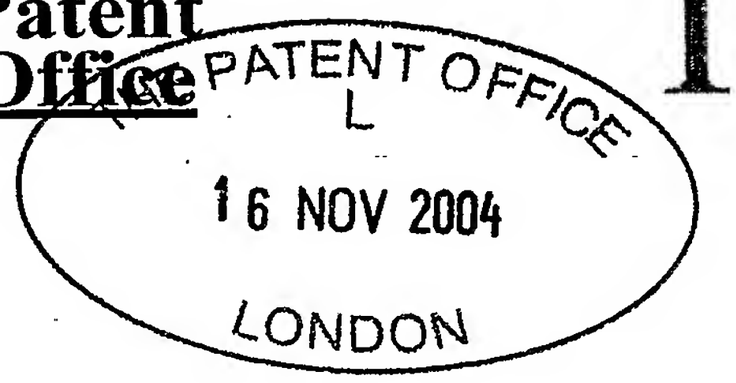

The Patent Office

Cardiff Road
Newport
South Wales
NP9 1RH

Request for grant of a patent

(See the notes on the back of this form. You can also get an explanatory leaflet from the Patent Office to help you fill in this form)

1. Your reference — RGC\P\14421.4GBA

2. Patent application number *(The Patent Office will fill in this part)* — 0425254.0

3. Full name, address and postcode of the or of each applicant *(underline all surnames)*

TISSUOMICS LIMITED
LAKIN ROSE, PIONEER HOUSE
VISION PARK
HISTON
CAMBRIDGE, CB4 9NL

Patents ADP number *(if you know it)* 8984650001

If the applicant is a corporate body, give the Country/state of its incorporation

4. Title of the invention — CHARACTERISING BODY TISSUES

5. Name of your agent *(if you have one)* — Olswang

"Address for service" in the United Kingdom to which all correspondence should be sent *(including the postcode)*

90 High Holborn
London, WC1V 6XX

Patents ADP number *(if you know it)* 76279915002

6. If you are declaring priority from one or more earlier patent applications, give the country and the date of filing of the or of each of these earlier applications and *(if you know it)* the or each application number

Country	Priority application number *(if you know)*	Date of filing *(day / month / year)*

7. If this application is divided or otherwise derived from an earlier UK application, give the number and the filing date of the earlier application

Number of earlier application	Date of filing *(day / month / year)*

8. Is a statement of inventorship and of right to grant of a patent required in support of this request? *(Answer 'Yes' if:*

a) any applicant named in part 3 is not an inventor, or
b) there is an inventor who is not named as an applicant, or
c) any named applicant is a corporate body.
See note (d))

Yes

Patents Form P1/77

1139181-1

Patents Form 1/77

9. Enter the number of sheets for any of the following items you are filing with this form. Do not count copies of the same document

Continuation sheets of this form	
Description	16
Claim(s)	0 DL
Abstract	0
Drawings	4 TH

10. If you are also filing any of the following, state how many against each item.

Priority documents	
Translations of priority documents	
Statement of inventorship and right to grant of a patent *(Patents Form 7/77)*	
Request for preliminary examination and search *(Patents Form 9/77)*	
Request for substantive examination *(Patents Form 10/77)*	
Any other documents *(please specify)*	

11. I/We request the grant of a patent on the basis of this application.

Signature [signature] Date 16 November 2004

12. Name and daytime telephone number of person to contact in the United Kingdom R. Carlin 0207 067 3000

Warning

After an application for a patent has been filed, the Comptroller of the Patent Office will consider whether publication or communication of the invention should be prohibited or restricted under Section 22 of the Patents Act 1977. You will be informed if it is necessary to prohibit or restrict your invention in this way. Furthermore, if you live in the United Kingdom, Section 23 of the Patents Act 1977 stops you from applying for a patent abroad without first getting written permission from the Patent Office unless an application has been filed at least 6 weeks beforehand in the United Kingdom for a patent for the same invention and either no direction prohibiting publication or communication has been given, or any such direction has been revoked.

Characterising Body Tissues

Field of the Invention

The present invention relates to methods for the characterisation of body tissue. More specifically, the invention is concerned with the characterisation of body tissue as normal (e.g. healthy) or abnormal (e.g. pathological). The invention has particular, although not necessarily exclusive, applicability to the diagnosis and management of cancer, including breast cancer.

Background

In order to manage suspected or overt breast cancer, tissue is removed from the patient in the form of a biopsy specimen and subjected to expert analysis by a histopathologist. This information leads to the disease management program for that patient. The analysis requires careful preparation of tissue samples that are then analysed by microscopy for prognostic parameters such as tumour size, type and grade. An important parameter in tissue classification is quantifying the constituent components present in the sample. Interpretation of the histology requires expertise that can only be learnt over many years based on a qualitative analysis of the tissue sample, which is a process prone to intra observer variability.

Despite the relative value of histopathological analysis, there remains a degree of imprecision in predicting tumour behaviour in the individual case. Additional techniques have the potential to fine-tune tissue characterisation to a greater degree than that currently used and hence will improve the targeted management of patients.

There remains in particular a need for techniques that can be used to characterise tissue to a greater degree *in vivo*, in order that the need for often painful and distressing biopsies can be reduced.

Summary of the Invention

In general terms the present invention is based on a recognition that Compton scattering densitometry techniques can be used in the analysis of body tissue to very effectively discriminate healthy and abnormal or diseased tissue and to discriminate types of abnormal tissue. Moreover, Compton scattering has been recognised as having potential for application to *in vivo* tissue characterisation techniques.

The invention provides a method for analysing and / or characterising body tissue, the method comprising:

obtaining Compton scatter data measured from a body tissue sample on which a penetrating (e.g. X-ray) radiation beam is incident; and

using the data to provide an analysis and/or characterisation of the tissue sample.

Compton scatter results from an interaction that occurs between a photon and an electron. For this interaction the electron is assumed to be unbound and acting as a free particle. This assumption can be made if the energy of the incident photon is much greater then the binding energy of the atom. Figure 1 illustrates the Compton interaction, where E_0 is the energy of the incident photon, E_1 is the energy of the scattered photon, m_0c^2 is the rest mass energy of the electron and θ is the scattering angle of the photon and φ is the scattering angle of the electron. T is the kinetic energy imparted to the electron.

The electron taking part in the interaction is assumed to be stationary, i.e. the initial energy (E_e) and momentum of the electron equals zero. During the interaction the photon imparts some of its energy to the electron. The amount of energy transferred determines the angle of the recoil of the electron and the angle of the resultant photon.

The angle and energy of a Compton scattered particle can be accurately calculated using the principle of conservation of energy and momentum. From Figure 1 it can be seen that the incident photon has energy $E_0 = h\nu$ and the scattered photon has energy $E_1 = h\nu'$. Resolving the energy and momentum into parallel and perpendicular components gives the important Compton scatter equation

$$E_1 = \frac{E_0}{1 + \left(\frac{E_0}{m_0c^2}\right)(1 - \cos\theta)}$$

hence a measure of Compton scatter can be made by detecting the appropriate energy photons at a given angle.

In some instances it may be sufficient for the Compton scatter data to be as simple as a count of photons detected at a selected angle/energy in a given time period. In other instances, it may be desirable to obtain an absolute measure of electron density (or some other derived measurement). Particularly in the latter case, the Compton scatter data is preferably corrected for attenuation in the tissue sample.

One way to compensate for attenuation effects is to use two radiation sources and two detectors. This is an approach commonly used in bone densitometry, but is less preferable when examining tissue samples, particularly *in vivo*, because it results in a greater dose of radiation.

A preferred method to correct for attenuation effects is to obtain data representing a measure of the directly transmitted x-ray radiation for each Compton scatter measurement. This data can then be used to correct the Compton scatter data for attenuation in the tissue sample.

Especially at low angles (less than 90°), it is also important to be able to distinguish Compton scatter measurement from the coherent scatter peak. So, where the transmitted radiation is to be used to correct for attenuation it is preferable that the energy of the scattered photons detected is as close as possible to that of the transmitted radiation. This ensures that the attenuation coefficients are not too different for the two measurements. The energy of the incident penetrating radiation beam and the angle selected for Compton scatter measurement are chosen such that the Compton and coherent scatter peaks can be resolved, whilst minimising the separation (i.e. energy) of these peaks. This substantially eliminates self-attenuation effects as it allows one to assume that the attenuation coefficients in the sample affecting both peaks are substantially the same.

Preferably the data is used as the input to a predefined calibration model that relates the Compton scatter data to one or more tissue characteristics (e.g. normal or abnormal). It is particularly preferred that the Compton scatter data is used as an input to a multivariate model as described in our co-pending UK patent application GB0328870.1

Brief Description of the Drawings

An embodiment of the invention is described below by way of example with reference to the accompanying drawings, in which:

Figure 1 illustrates the cylindrical geometry used as the sample holder for the measurement of the electron density;

Figure 2 illustrates the experimental configuration for the Compton scatter measurements;

Figure 3 shows a scatter spectrum from a malignant breast tissue sample;

Figure 4 shows a calibration graph of the calculated linear scatter coefficients against the counts measured in the Compton scatter peak for the calibration solutions;

Figure 5 shows a graph of the differential scatter coefficient from experimental data against the calculated electron density for the calibration solutions;

Figure 6 shows a box plot of the electron density results obtained from the tissue samples; and

Figure 7 shows a graph of the electron density values for each tissue type.

Description of Embodiments

The invention is exemplified below with reference to *in vitro* Compton scatter measurements from uniform samples of body tissue. The general technique is, however, equally applicable to the analysis of non-uniform tissue samples, including *in vivo* applications.

The experiment was undertaken in two sections; Compton scatter measurements were made on all the samples, followed by transmission measurements. This was done in preference to the two measurements being made consecutively for each sample. This method was adopted for two reasons; firstly to ensure consistency of set-up between samples through minimising the moving of equipment and secondly to save time.

Material and Methods

Theory

The angle and energy of a Compton scattered particle can be accurately calculated using the principle of conservation of energy and momentum. If the incident photon has energy $E_1 = h\nu$ and the scattered photon has energy $E_2 = h\nu'$. Resolving the energy and momentum into parallel and perpendicular components gives the important Compton equation

$$E_2 = \frac{E_1}{1 + \left(\frac{E_1}{m_0 c^2}\right)(1 - \cos\theta)} \qquad (1)$$

where $m_0 c^2$ is the rest mass energy of the electron and θ is the scattered angle.

Consider the cylindrical geometry shown in figure 1. A beam of photons is in the direction AB with energy E_1 and a detector is placed at a scatter angle θ to the incident beam. The number of scattered photons, S, with energy E_2 reaching the detector is given by

$$S \propto (V\rho_e)\exp\left(-\int_A^B \mu_1(x)dx\right)\exp\left(-\int_B^{B'} \mu_2(x)dx\right) \qquad (2)$$

where V is the volume of scattering material, ρ_e is the electron density of the material in the scattering volume, μ_1 is the attenuation coefficient of photons at the incident energy, and μ_2 is the attenuation coefficient of the Compton photons, scattered through angle θ with reduced energy E_2. If the incident energy E_1 and scatter angle θ are carefully chosen it can be assumed that $E_1 \approx E_2$ and therefore that $\mu_1 \approx \mu_2$. Using these assumptions it follows that

$$\exp\left(-\int_A^B \mu_1(x)dx\right)\exp\left(-\int_B^{B'} \mu_2(x)dx\right) \approx \exp\left(-\int_A^{B'} \mu_1(x)dx\right) \qquad (3)$$

and equation (2) becomes

$$S \propto (V\rho_e)\exp\left(-\int_A^{B'} \mu_1(x)dx\right) \qquad (4)$$

From the exponential law of attenuation it is found that

$$\frac{I}{I_0} = \exp\left(-\int \mu_1(x)dx\right) \qquad (5)$$

where I_0 is the incident photon intensity and I is the transmitted photon intensity.

Therefore by obtaining a measure of I_0, I and S, the electron density can be found from

$$\rho_e = k\left(\frac{S}{T}\right) \qquad (6)$$

where S is the scattered count intensity, $T=I/I_0$ and k is a constant which includes the volume term determined using calibration materials with known electron densities.

Samples

A sample set of four different tissue types were examined comprising of 5 fibroadenoma (benign), 8 invasive ductal carcinomas (malignant), 4 fibrocystic change (non-malignant abnormal) and 5 pure adipose (normal) samples. Each sample was examined at two

points. The samples were placed into polythene sample vials of 6mm inside diameter and 1mm wall thickness. Although the walls of the vial were relatively thick and would cause some attenuation of the scattered beam, these containers were chosen because they offered a number of important advantages.

The sides were completely rigid so the samples could be placed into a vial and lightly compressed with a stopper without it distorting. This stopper is to remove any air gaps and it also minimises tissue movement throughout the experiment. The containers were cheap so each sample could have its own holder for the duration of the experiment, making it possible to move the sample and reposition it accurately. The samples also needed to be symmetrical about a centre of rotation.

Method

The Kα characteristic lines produced by a tungsten target x-ray tube were utilized as a monoenergetic source to ensure that the Compton scatter peak was detectable. Using this method the Compton and coherent scattered peaks from a recorded spectrum can be easily resolved and windowed and the bremsstrahlung background subtracted. The desired outcome of the experiment was to be able to resolve the Compton and coherent scattered peaks, whilst keeping them as close in energy as possible. The detector characteristics dictated that the minimum resolvable energy is about 1 keV.

The experimental set-up is shown in figure 2. The x-ray beam was collimated to 0.5mm diameter, both before and after the sample. This was the smallest beam size viable whilst maintaining a reasonable flux. The K_α line from the tungsten target of the x-ray source ($E_{k\alpha 2}$=57.97 keV) was used. At this energy a scattering angle of 30° gave a peak separation of 1 keV between the Compton and coherent scatter peaks. The scattering volume comprises of the tissue contained within the intersecting area of the incident and scattered beam. For this beam collimation and scattering angle the entire scattering volume was contained within the sample, with no air or polythene from the vial included. Each sample was measured for a total time of four hours, with the sample being rotated throughout the measurement in order to reduce any errors due to the inhomogeneity of the tissues.

Equipment

The experiments were performed using a Pantak HF160 industrial x-ray tube. An HPGe detector was used in order to produce the energy resolution required to resolve the Compton and coherent peaks. The energy resolution was measured to be 0.435 keV at

59.54 keV (0.73%). The detector was connected via a pre-amp and an amplifier to two single channel analysers, one to record the Compton peak and one to record a background region. An observed scatter spectrum of a malignant tissue is shown in figure 3.

The two coherent peaks of the $K_{\alpha 1}$ and $K_{\alpha 2}$ W lines can be identified and the two smaller Compton scatter peaks can be seen. The $K_{\alpha 2}$ Compton peak was windowed over an area where there was no superposition of the $K_{\alpha 2}$ coherent peak. This windowed area, which was used for the scatter measurements, is also shown in figure 3. The transmission measurements for each sample were made by placing the detector at zero degrees and recording the photon intensity with and without a sample in position in the beam.

System calibration

As the composition of the tissues being measured is unknown, the electron density measurement system needed to be calibrated. This was carried out by measuring substances with a known electron density or one that could be calculated. Five substances were chosen in order to produce a calibration curve.

The solutions chosen were water, iso-propanol, and solutions of potassium hydrogen phosphate K_2HPO_4. Water and propanol were chosen because they are readily available, easy to handle and have a known electron density that is close to that of biological materials. The concentration of the phosphate solutions could be varied to provide solutions with differing electron densities. In order to have values close to that of tissue, solutions of 2%, 5% and 10% were used.

In order to verify the scatter data for the calibration solutions the linear differential scattering coefficient can be calculated theoretically as the composition of these solutions is known. The linear scattering coefficient is a measure of the probability that a photon of incident energy E will be scattered through an angle θ and is given by equation (7):

$$\mu_{Compton} = \rho N_A \frac{S(x)}{M} \frac{d\sigma_{KN}}{d\Omega} \qquad (7)$$

$$where \frac{S}{M} = \sum_i \frac{S_i(x)}{m_i} \omega_i \qquad (8)$$

where M is the molecular mass of the material, ρ is the mass density; and N_A is Avogadro's constant. S(x) is the incoherent scattering factor and the differential scattering cross section is denoted with KN for the Klein-Nishina cross section. The Klein-Nishina differential scattering cross section for the Compton effect is given by

$$\frac{d\sigma_{KN}}{d\Omega} = r_0^2\left[\frac{1}{1+\alpha(1-\cos\theta)}\right]^3\left[\frac{1+\cos\theta}{2}\right]\left[1+\frac{\alpha^2(1-\cos\theta)^2}{(1+\cos^2\theta)[1+\alpha(1-\cos\theta)]}\right] \qquad (9)$$

where E is the incident photon energy and θ is the photon scattering angle. α is the ratio of the incident photon energy to the electron rest mass energy given by

$$\alpha = \frac{E}{m_0c^2} \qquad (10)$$

and r_0 is the classical electron radius.

The Klein-Nishina differential scattering cross section is dependent on photon energy and the angle of scatter. It was calculated to be 7.177 x 10^{-26} cm^2/electron for 57.97 keV photons at a 30° scattering angle. Using this value and tabulated values for S(x) taken from Hubbell *et al.* (1975) a value for $\mu_{Compton}$ for each calibration solution was calculated. A graph showing the experimental scatter measurements against the scatter coefficient values calculated from equation (7) is shown in figure 4.

The corrected scatter counts are the counts measured in the scatter peak corrected for attenuation and are given by

$$S_{corr} = \frac{[S_{meas} - B_s]}{\left[\left(\frac{I_{meas} - B_T}{I_0 - B_0}\right)\right]} \qquad (11)$$

where S_{corr} is the counts recorded in the scatter peak corrected for attenuation. S_{meas} is the number of counts in the scatter peak, B_s is the background counts in the scatter peak, I_{meas} is the number of counts in the transmitted peak, B_T is the number of

background counts in the transmitted peak, I_0 is the unattenuated count intensity and B_0 is the background area for these counts. Figure 4 can be used to convert the corrected counts measured into differential scatter coefficients for Compton scatter, μ_s, where

$$\mu_s = k[S_{corr}] + N \qquad (12)$$

In equation (12) S_{corr} is the corrected scatter counts as described in equation (11), N is the systematic experimental error and k is a constant that is found using the calibration curve.

As the composition of the calibration solutions are known the electron densities of these solutions can be calculated using the following formula

$$\rho_e = \rho N_A \sum \frac{Z_i}{A_i} \varpi_i \qquad (13)$$

where ρ is the physical density of the material and Z/A is the ratio of atomic number to atomic weight for each element of mass fraction ω. Z/A values are tabulated and were taken from (Attix 1986). Figure 5 shows the theoretical electron densities calculated from equation (13) plotted against the measured scattering coefficients given by equation (12). It can be seen that the two quantities correlate well with a gradient equal to the Klein-Nishina cross section which is expected, as for high values of x the incoherent scattering factors become equal to Z.

Results

Figure 6 shows the results of the electron density measurements that were obtained from two points on each sample. The median of each tissue type is shown (thick middle line). The interquartile range is contained within the box and the whiskers show the total range.

The graph of figure 4 gives a calibration equation to convert the number of counts in the corrected scatter peak into the differential linear scatter coefficient μ_s. The equation given by the graph is

$$\mu_s = 1.737 \times 10^{-7} x + 7.919 \times 10^{-3} \qquad (14)$$

where x is the corrected counts in the Compton peak.

These experimental scatter coefficients are then converted into electron densities using the Klein-Nishina cross section. This conversion is shown by the trend line in figure 5. The average results are shown in figure 7.

In figure 7 the values of electron density for standard tissue compositions given in ICRU report 44 (ICRU 1989) are also displayed. In this report three separate values are given for different tissue compositions. The elemental compositions of these six tissues have been given in table 1. It is worth noting that the values quoted in this report are for healthy tissues only, as there is no published data for malignant tissue growths.

Tissue	H	C	N	O	Other
Adipose #1	11.2	51.7	1.3	35.5	0.1 Na, 0.1 S, 0.1 Cl
Adipose #2	11.4	59.8	0.7	27.8	0.1 Na, 0.1 S, 0.1 Cl
Adipose #3	11.6	68.1	0.2	19.8	0.1 Na, 0.2 S, 0.1 Cl
Glandular #1	10.9	50.6	2.3	35.8	0.1 Na, 0.1 P, 0.1 S, 0.1 Cl
Glandular #2	10.6	33.2	3	52.7	0.1 Na, 0.1 P, 0.2 S, 0.1 Cl
Glandular #3	10.2	15.8	3.7	69.8	0.1 Na, 0.1 P, 0.2 S, 0.1 Cl

Table 1. The elemental compositions (percentage by mass) of adult tissues (ICRU Report 44, 1989)

It is usually assumed that malignant tissue has approximately the same structure as healthy glandular tissue. This is because tumours are usually within fibrous tissue rather than growing in purely fatty (adipose) tissue.

The final results obtained are displayed in table 2.

Tissue	Electron density (e/cm^3)
Benign	$(3.330 \pm 0.140) \times 10^{23}$
Malignant	$(3.490 \pm 0.147) \times 10^{23}$
Adipose	$(3.281 \pm 0.138) \times 10^{23}$
Fibrocystic change	$(3.752 \pm 0.158) \times 10^{23}$

Table 2. *Experimental values obtained for tissue electron densities*

Each individual measurement is subject to statistical variation. The error σ is given as: $\sigma = \sqrt{\frac{\overline{x}}{N}}$ where $\overline{x}$ is the mean number of counts if the reading is repeated N times.

For the scatter readings each measurement was measured for a sufficient time (4 hours) to ensure that the error on the counts was sufficiently low (<0.5%). Due to time constraints the readings were not repeated.

The largest error is associated with the subtraction of the background counts. The overall error on the background count calculation is 4.2%. This is shown by the error bars in figure 4. Other sources of error are the effect of multiple scatter, the error in positioning and the error in repositioning the sample for the transmission measurements. There is also a widening of the Compton scatter peak caused by the acceptance angle of the pre-detector collimator. None of these other errors have been considered as they are difficult to quantify and are small compared to the background subtraction error outlined above.

Discussion and Conclusions

The results show that there is a detectable difference between the electron density of adipose and malignant tissue, to a value of 6.4%. This difference is consistent with the values found by using the adipose and glandular tissue values from ICRU report 44. The average value for glandular tissue (ICRU44 glandular#2) is 6.2% higher than the average adipose value (ICRU44 adipose #2).

There has been no composition values published for benign (fibroadenoma) or fibrocystic tissues. However the measurements made within this study found a difference in the electron density of benign and malignant tissues to the value of 5.6% and a difference between fibrocystic change and malignant tissue to be 2.3%.

It is difficult to verify these results using the literature as there is no published data from any previous studies using this tissue type. However the high degree of correlation for the calibration solutions (figure 4) shows that the system has a reliable accuracy. This inspires confidence in the findings that there is a measurable difference between the benign and malignant tissues.

There is a great deal of evidence to suggest that the metabolism and physiology of tumour cells differ greatly to that of normal and indeed benign cells.

Within a benign tumour growth there is often an increase in cell proliferation but the cells themselves are relatively normal. However, in a malignant lesion the structure and metabolism of the tumour cells and host tissue have a different biochemical structure (Gould 1997). This implies that the increase in the electron density of benign tissues compare to normal may potentially be due to an increase in cell concentration rather than to changes in composition, as seen in malignant tissues. This is consistent with the finding that benign tissues *ex-vivo* have an electron density which is only slightly higher than normal tissues and malignant tissues display a much larger difference.

Dr Otto Warburg first observed in 1930 that cancer cells have a fundamentally different energy metabolism than normal cells (Warberg 1930). Since then research has shown that tumour cells undergo anaerobic glycolysis, the process where glucose is converted to lactic acid through the process of fermentation. This process is extremely inefficient compared to normal cell aerobic respiration.

Glucose consumption rate has been shown to be proportional to histological grade (Vaupel *et al.* 1989) and high grade tumours can absorb about 40 times more glucose in order to supply their high energy demands for increased growth. This process is what

makes positron emission tomography (PET) imaging so effective at imaging tumours using 18F-FDG, an analogue of glucose. It enables PET to distinguish between benign and malignant neoplasms with a high degree of accuracy, as benign tissues do not exhibit increased glucose consumption (Brock *et al.* 1997).

Anaerobic glycolysis causes a build up of lactic acid to occur within the tissue. The lactic acid (CH3-CH(OH)-CO(OH)) which builds up within the tumour has a high electron density compared to the host tissue of 8.2×10^{23} electrons/cm^3 and so could be responsible for the increase in electron density that is measured. There is also an increase of ketones and glutamine (Vaupel *et al.* 1989) which may also increase the overall electron density of tumour tissues. Although no direct measurements have been made of the composition of benign and malignant tissues, the above suggests that there are significant differences in composition. It is difficult to estimate the precise nature of the composition changes, given that there are a number of processes occurring in the tissue during tumourgenesis.

The final tissue type that was examined was fibrocystic change. Although this term encompasses a range of histological changes, the majority are characterised by tissue fibrosis. This is a scarring process whereby the stromal (connective tissue) component of the tissue is increased and collagen accumulates. Although increased mature collagen may be seen in a few other benign disease processes in the breast, the most pronounced increase probably occurs during fibrocystic change. This may account for the finding that this tissue classification had a higher electron density than any other type of tissue, even malignancy. When examining the tissues exhibiting fibrocystic change it is likely that any fluid filled pockets (cysts) will become dispersed during tissue preparation leaving only the dense fibrotic tissue under examination.

Not only is the present invention useful for assessing increased numbers of fibroadenomas, invasive ductal carcinomas and FCC tissues, the present invention may also be adapted to assess healthy fibrous tissue and further disease processes.

References

Al-Bahri J S and Spyrou N M 1998 Electron density of normal and pathological breast tissues using a Compton scattering technique *Applied Radiation and Isotopes* **49** 1677-1684

Attix F 1986 *Introduction to radiological physics and radiation dosimetry* (New York: Wiley and Sons)

Avtandilov G, Dembo A, Komardin O, Lazarev P, Paukshto M, Shkolnik L, and Zayratiyants O 2000 Human tissue analysis by small-angle X-ray scattering *Journal of Applied Crystallography* **33** 511-514

Brock C S, Meikle S R, and Price P 1997 Does fluorine-18 fluorodeoxyglucose metabolic imaging of tumours benefit oncology? *European Journal of Nuclear Medicine* **24** 691-705

Department of Health. NHS Breast Screening Programme Annual Review. 2003. Report

Duke P R and Hanson J A 1984 Compton Scatter Densitometry with Polychromatic Sources *Medical Physics* **11** 624-632

Evans S H, Bradley D A, Dance D R, Bateman J E, and Jones C H 1991 Measurement of Small-Angle Photon Scattering for Some Breast Tissues and Tissue Substitute Materials *Physics in Medicine and Biology* **36** 7-18

Farquharson M J and Geraki K 2004 The use of combined trace element XRF and EDXRD data as a histopathology tool using a multivariate analysis approach in characterizing breast tissue *X-Ray Spectrometry. In press*

Fernandez M, Keyrilainen J, Serimaa R, Torkkeli M, Karjalainen-Lindsberg M L, Tenhunen M, Thomlinson W, Urban V, and Suortti P 2002 Small-angle x-ray scattering studies of human breast tissue samples *Physics in Medicine and Biology* **47** 577-592

Geraki K, Farquharson M J, and Bradley D A 2004 X-ray fluorescence and energy dispersive x-ray diffraction for the quantification of elemental concentrations in breast tissue *Physics in Medicine and Biology* **49** 99-110

Gould B 1997 *Pathophysiology for the Health Professions* (Pensylvania: WB Saunders)

Hubbell J, Viegele Wm J, Briggs E A, Brown R T, Cromer D T, and Howerton R J 1975 Atomic Form Factors, Incoherent Scattering Functions and Photon Scattering Cross Sections *Journal of Physical and Chemical Reference Data* **4** 471-616

ICRU. Tissue Substitutes in Radiation Dosimetry and Measurement, Report 44. 1989. Maryland, International Commission on Radiation Units and Measurements. Report

Johns P C and Yaffe M J 1983 Coherent Scatter in Diagnostic-Radiology *Medical Physics* **10** 40-50

Kidane G, Speller R D, Royle G J, and Hanby A M 1999 X-ray scatter signatures for normal and neoplastic breast tissues *Physics in Medicine and Biology* **44** 1791-1802

Kosanetzky J, Knoerr B, Harding G, and Neitzel U 1987 X-Ray-Diffraction Measurements of Some Plastic Materials and Body-Tissues *Medical Physics* **14** 526-532

Lewis R A, Rogers K D, Hall C J, Towns-Andrews E, Slawson S, Evans A, Pinder S E, Ellis I O, Boggis C R M, Hufton A P, and Dance D R 2000 Breast cancer diagnosis using scattered X-rays *Journal of Synchrotron Radiation* **7** 348-352

Morin L R M 1982 Molecular-Form Factors and Photon Coherent Scattering Cross-Sections of Water *Journal of Physical and Chemical Reference Data* **11** 1091-1098

Narten A H and Levy H A 1971 Liquid Water: Molecular Correlation Functions from X-Ray Diffraction *Journal of Chemical Physics* **55** 2263-2269

Olkkonen H and Karjalainen P 1975 A Tm-170 gamma scattering technique for the determination of absolute bone density *British Journal of Radiology* **48** 594-597

Peplow D E and Verghese K 1998 Measured molecular coherent scattering form factors of animal tissues, plastics and human breast tissue *Physics in Medicine and Biology* **43** 2431-2452

Poletti M E, Goncalves O D, and Mazzaro I 2002 X-ray scattering from human breast tissues and breast- equivalent materials *Physics in Medicine and Biology* **47** 47-63

Speller R D, Royle G J, and Horrocks J A 1989 Instrumentation and Techniques in Bone-Density Measurement *Journal of Physics E-Scientific Instruments* **22** 202-214

Tartari A, Casnati E, Bonifazzi C, and Baraldi C 1997 Molecular differential cross sections for x-ray coherent scattering in fat and polymethyl methacrylate *Physics in Medicine and Biology* **42** 2551-2560

Vaupel P, Kallinowski F, and Okunieff P 1989 Blood-Flow, Oxygen and Nutrient Supply, and Metabolic Microenvironment of Human-Tumors - A Review *Cancer Research* **49** 6449-6465

Warberg O 1930 *The metabolism of tumours* (London: Constable)

Webber C E and Kennet T J 1976 Bone Density Measured by Photon Scattering. I. A System for Clinical Use *Physics in Medicine and Biology* **21** 760-769

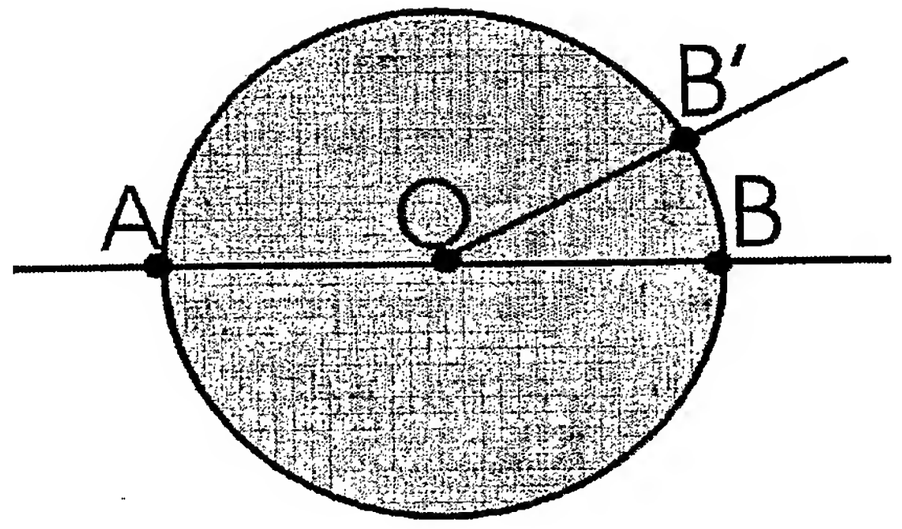
B′
A
O
B

Fig 1

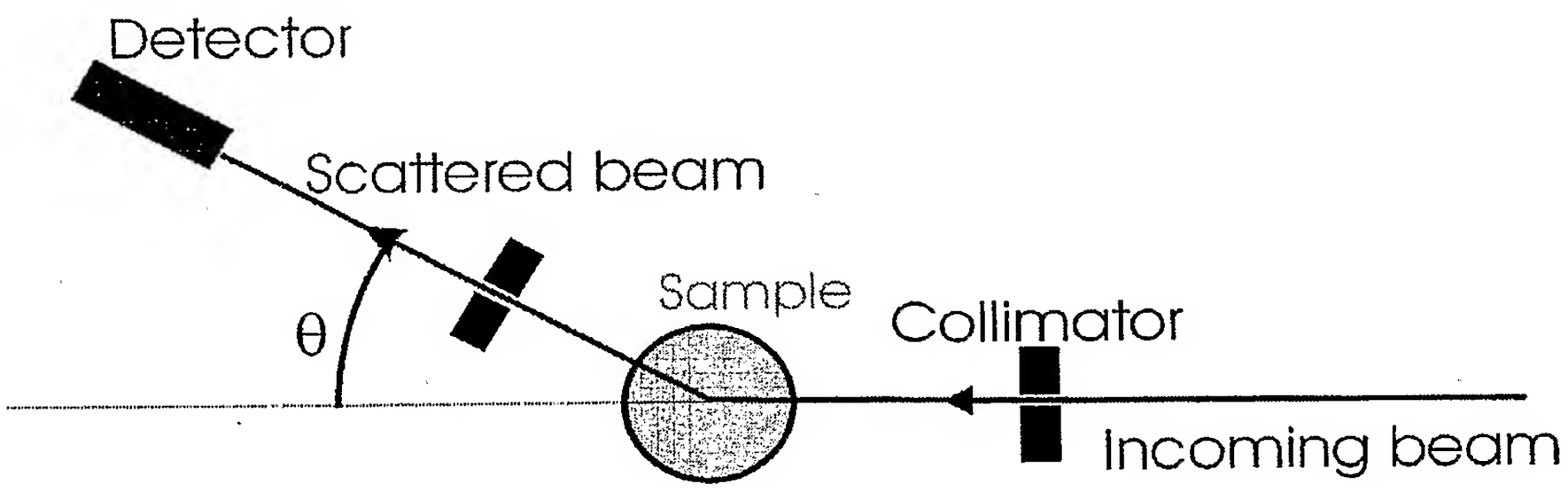
Detector
Scattered beam
θ
Sample
Collimator
Incoming beam

Fig 2

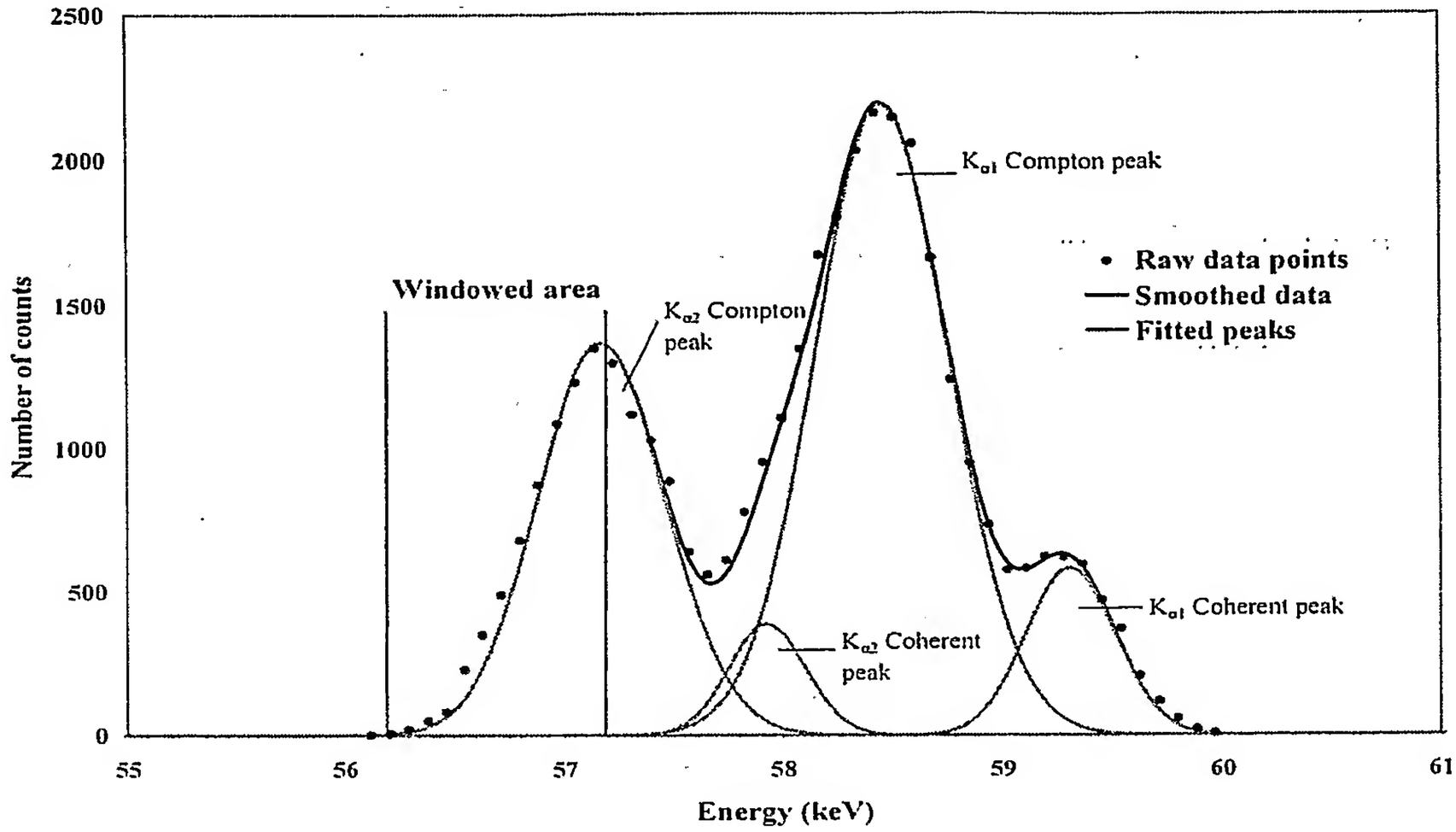
2500
2000
1500
1000
500
0
Number of counts
55
56
57
58
59
60
61
Energy (keV)
Windowed area
$K_{\alpha 2}$ Compton peak
$K_{\alpha 1}$ Compton peak
$K_{\alpha 1}$ Coherent peak
$K_{\alpha 2}$ Coherent peak
Raw data points
Smoothed data
Fitted peaks

Fig 3

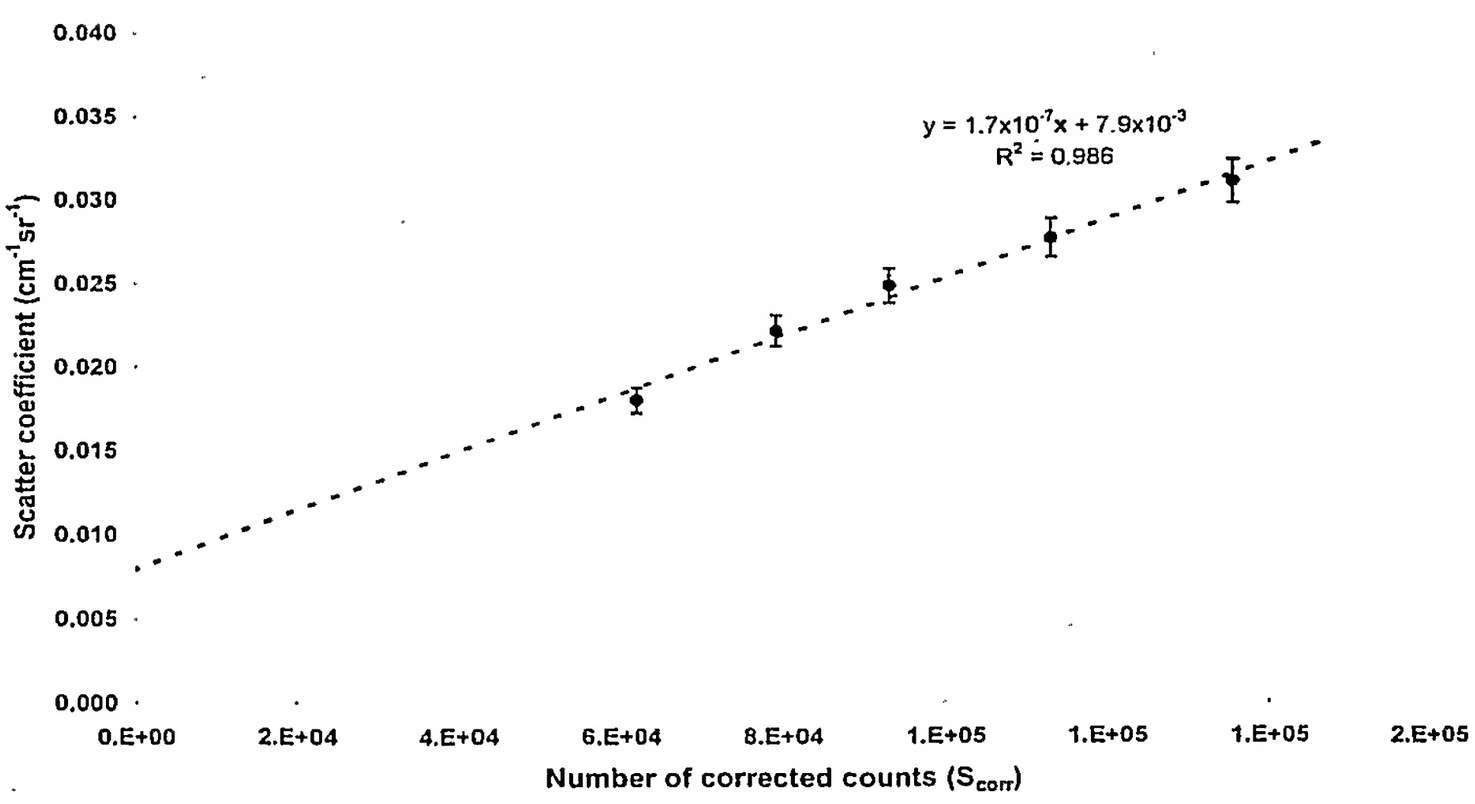
0.040
0.035
0.030
0.025
0.020
0.015
0.010
0.005
0.000
Scatter coefficient ($cm^{-1}sr^{-1}$)
0.E+00
2.E+04
4.E+04
6.E+04
8.E+04
1.E+05
1.E+05
1.E+05
2.E+05
Number of corrected counts (S_{corr})
$y = 1.7x10^{-7}x + 7.9x10^{-3}$
$R^2 = 0.986$

Fig 4

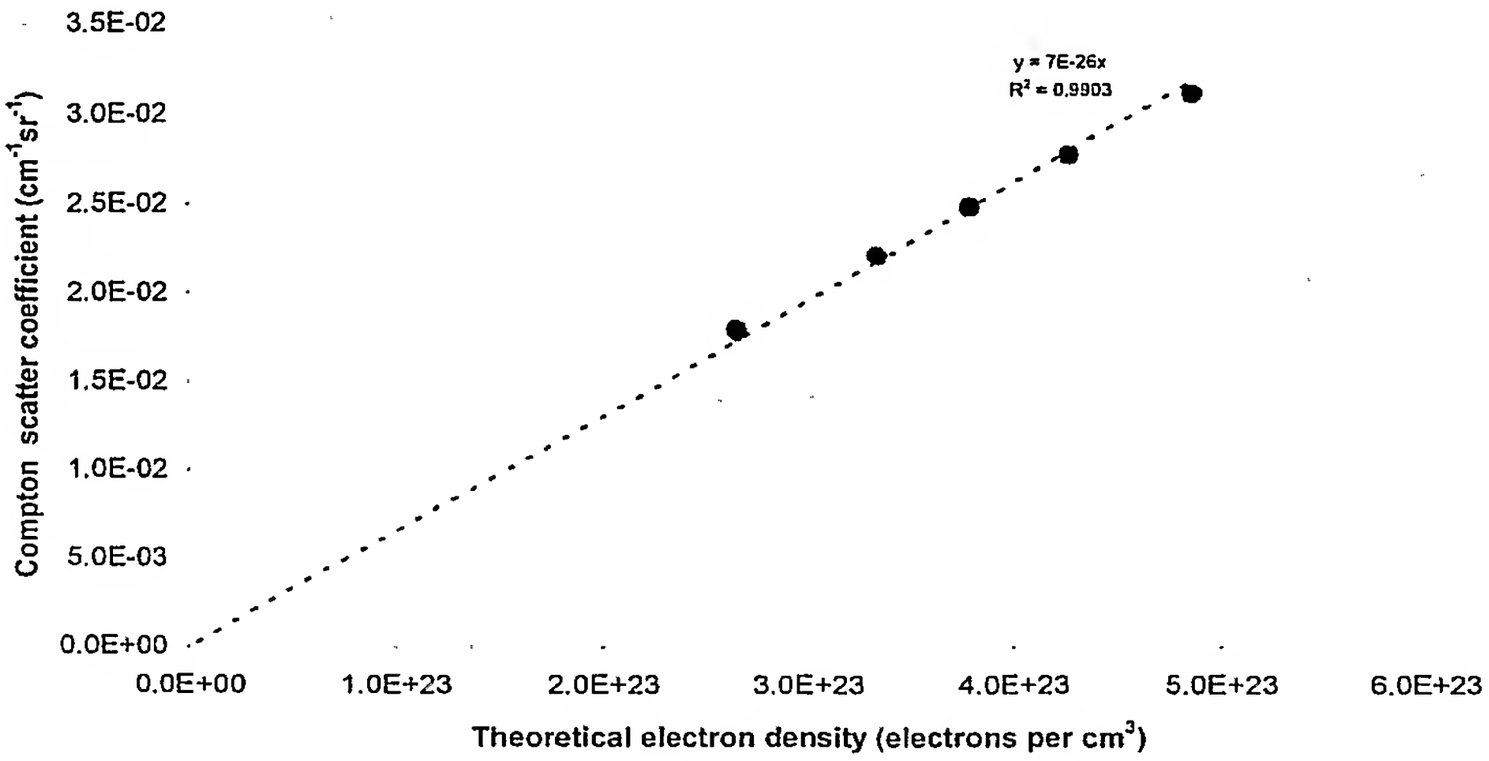
y = 7E-26x
R² = 0,9903
Compton scatter coefficient (cm⁻¹sr⁻¹)
3.5E-02
3.0E-02
2.5E-02
2.0E-02
1.5E-02
1.0E-02
5.0E-03
0.0E+00
0.0E+00
1.0E+23
2.0E+23
3.0E+23
4.0E+23
5.0E+23
6.0E+23
Theoretical electron density (electrons per cm³)

Fig 5

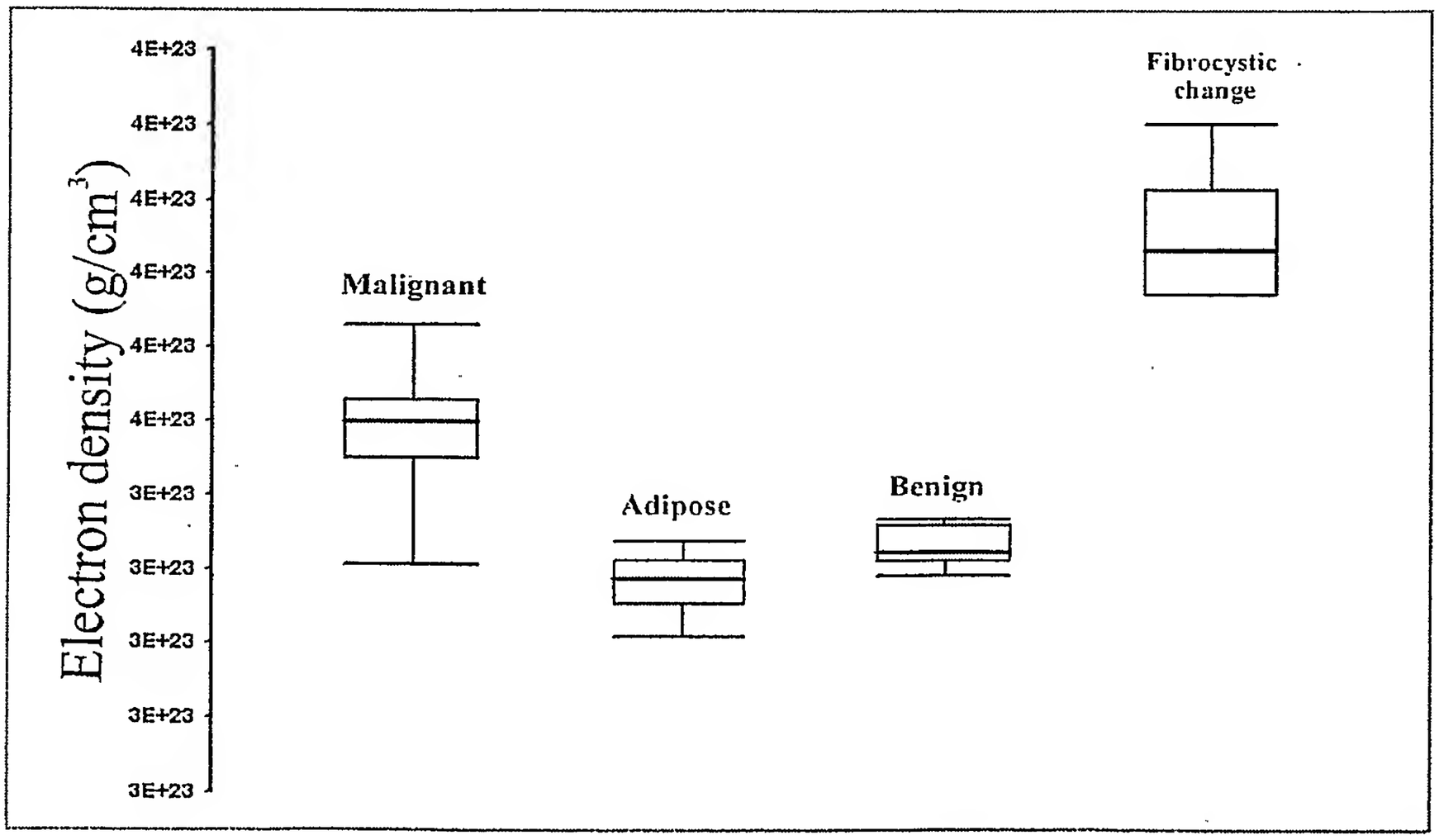
Electron density (g/cm³)
4E+23
4E+23
4E+23
4E+23
4E+23
4E+23
3E+23
3E+23
3E+23
3E+23
3E+23
Malignant
Fibrocystic change
Adipose
Benign

Fig 6

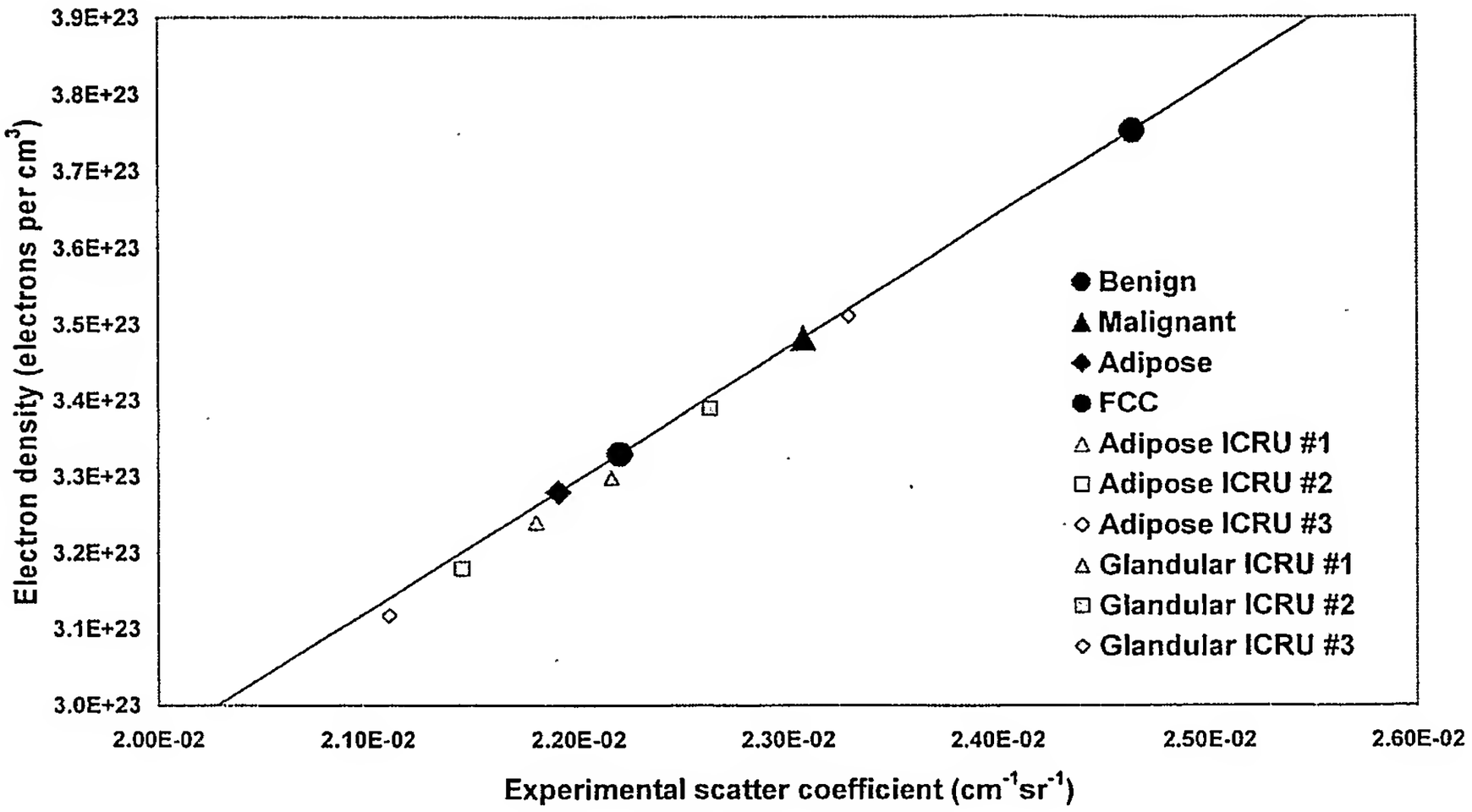
3.9E+23
3.8E+23
3.7E+23
3.6E+23
3.5E+23
3.4E+23
3.3E+23
3.2E+23
3.1E+23
3.0E+23
Electron density (electrons per cm3)
2.00E-02
2.10E-02
2.20E-02
2.30E-02
2.40E-02
2.50E-02
2.60E-02
Experimental scatter coefficient (cm-1sr-1)
Benign
Malignant
Adipose
FCC
Adipose ICRU #1
Adipose ICRU #2
Adipose ICRU #3
Glandular ICRU #1
Glandular ICRU #2
Glandular ICRU #3

Fig 7